Low Reynolds Number Airfoils for Small Horizontal Axis
Wind Turbines

by

Philippe Giguère and Michael S. Selig

Low Reynolds Number Airfoils for Small Horizontal Axis Wind Turbines

Philippe Giguère[1] and Michael S. Selig[2]

Department of Aeronautical and Astronautical Engineering, University of Illinois at Urbana-Champaign, 306 Talbot Laboratory, 104 S. Wright St, Urbana, Illinois 61801-2935. (217) 244-5757, giguere@uiuc.edu, m-selig@uiuc.edu

ABSTRACT

To facilitate the airfoil selection process for small horizontal-axis wind turbines, an extensive database of low Reynolds number airfoils has been generated. The database, which consists of lift and drag data, was obtained from experiments conducted in the same wind tunnel testing facility. Experiments with simulated leading-edge roughness were also performed to model the effect of blade erosion and the accumulation of roughness elements, such as insect debris, on airfoil performance. Based on the lift curves and drag polars, guidelines that should be useful in selecting appropriate airfoils for particular blade designs are given. Some of these guidelines are also applicable to larger HAWTs.

NOMENCLATURE

a	Axial induction factor
c	Chord length
C_d	Drag coefficient
C_l	Lift coefficient
R	Blade radius
$\Re$	Reduced chord Reynolds number
r	Radial distance from center of rotation
Re	Chord Reynolds number
TSR	Tip-speed ratio
V	Relative velocity at a given blade station
V_∞	Wind or freestream velocity
α	Angle of attack
v	Kinematic viscosity
Ω	Rotational velocity

1. INTRODUCTION

For small horizontal-axis wind turbines (HAWTs), the rotor blades usually operate at low Reynolds numbers along the entire span. The unusual aerodynamic characteristics associated with low Reynolds number airfoil aerodynamics can severely degrade the performance of small HAWTs if the selected airfoils are not suitable for low Reynolds number applications. Consequently, the airfoil selection is a particularly critical aspect of the blade design process of small HAWTS.

Traditional airfoils, such as the NACA airfoils,[1] were designed to operate at high Reynolds numbers since they were mainly intended for full-scale aircraft. At high Reynolds numbers, boundary layer transition takes place before laminar separation, thereby avoiding the peculiarities of low Reynolds number aerodynamics. In contrast, the behavior of the boundary layer is much different at low Reynolds numbers where laminar separation is predominant (subcritical flow regime). Traditional airfoils generally exhibit poor performance at low Reynolds numbers because of laminar separation effects. Therefore, optimum aerodynamic performance of

---

[1]Graduate Research Assistant; [2]Assistant Professor

small HAWTs is found through the use of airfoils designed for this subcritical flow regime, i.e. low Reynolds number airfoils.

Only a few low Reynolds number airfoils have been designed specifically for small HAWTs. For example, there is an NREL thick airfoil family for small blades that includes two airfoils mainly intended for stall-regulated wind turbines,[2] and four airfoils were recently specifically designed for small variable-speed HAWTs having rated power between 1–5 kW.[3] (These four airfoils, while not discussed here, are documented in Reference 3). Despite the limited number of airfoils specially designed for small blades, the variety of existing low Reynolds number airfoils documented in the literature offers a large selection of airfoils for small HAWTs.[4-10] Unfortunately, the effects of leading-edge roughness are rarely documented and results obtained from various wind tunnel facilities do not provide the best basis for comparison.[10] Also, despite the recent improvements in computational airfoil aerodynamics,[11] the accuracy of computational results is questionable in the low Reynolds numbers regime. Most notably, the laminar separation bubble drag is usually underpredicted.[8] Accordingly, to support the blade design process of small wind turbines, there has been a need for a database of low Reynolds number airfoil data under clean and rough conditions, originating preferably from the same wind tunnel facility.

In an effort to provide an extensive airfoil database for use in small HAWT blade design and optimization studies, the results obtained from a large scale wind tunnel testing program at the University of Illinois[6-8] were analyzed to find the most promising low Reynolds number airfoils for wind turbine applications. A total of 15 airfoils, including three airfoils specifically designed for small HAWTs, are documented in this paper and eight of them were also tested with simulated roughness at the leading edge. The 15 airfoils have been classified for each of the different modes of operation of a wind turbine: variable-speed (variable rpm), variable-pitch and stall regulated (both constant rpm). A brief review of low Reynolds number airfoil aerodynamics is provided before presenting the wind tunnel test results. The analysis of the wind tunnel data provides guidelines for use in selecting appropriate airfoils for particular blade designs.

2. LOW REYNOLDS NUMBER AIRFOIL AERODYNAMICS

Before presenting and discussing the airfoil data, it seems worthwhile to briefly review the underlying characteristics of low Reynolds number airfoil aerodynamics.[9,12] The low Reynolds number regime can be defined as that for which laminar separation dominates the drag. Therefore, the Reynolds number range that defines this subcritical flow regime is airfoil dependent. For example, thick airfoils and those designed for higher Reynolds numbers usually have an undesirably wider Reynolds number range for which the flow is subcritical as compared with thin and low Reynolds number airfoils. Even though there is no fixed Reynolds number range that bounds the low Reynolds number regime, the term low Reynolds number has also come to mean the flow regime where the chord Reynolds number is below approximately 500,000. This is why small HAWTs are said to usually operate at low Reynolds numbers independently of the airfoil(s) used on the blades.

At low Reynolds numbers, turbulent reattachment usually follows laminar separation, thereby forming the so-called laminar separation bubble. Most of the unusual aerodynamic characteristics at low Reynolds numbers can be traced to the presence and behavior of a laminar separation bubble on the airfoil. The length and behavior of the laminar separation bubble is airfoil, Reynolds number, and angle of attack dependent, typically moving toward the leading edge with increasing angle of attack.

An increase in drag followed by a reduction in drag for higher lift coefficients, that is a drag polar with a "high-drag knee," is indicative of the presence of a laminar separation bubble on the airfoil. The effects are usually particularly severe at a chord Reynolds number below 200,000 where a large and rapid increase in drag is frequent, and where the bubble may burst prematurely. Such a bursting phenomenon causes an even larger increase in drag and a discontinuity on the lift-curve slope. The behavior of the laminar separation bubble may be also such that the lift coefficient at a given angle of attack depends on the direction from which the angle of attack was reached. This leads to aerodynamic hysteresis that can be traced to the bursting of the laminar separation bubble or its transition from a long bubble to a shorter one.[9]

From the above discussion, it is clear that minimizing the effects of laminar separation bubbles is of great importance at low Reynolds numbers. One method of reducing the drag caused by a laminar separation bubble (bubble drag) is to promote early transition on the airfoil through the use of a mechanical turbulator or a trip. This method to reduce laminar separation effects is the only one available to existing airfoils and requires some experience in selecting the proper location and thickness of the trip to maximise the reduction in bubble drag and minimize the device drag.[13] Another method, however, is to design the airfoil with a very gradual upper-surface pressure recovery (bubble ramp) to minimize the bubble drag. Most modern low Reynolds number airfoils are designed following this approach, that often provides lower drag and higher maximum lift-to-drag ratios as compared with those of traditional airfoils. Consequently, low Reynolds number airfoils are good candidates for small HAWTs to enhance aerodynamic blade performance and thus, energy production.

3. THE AIRFOILS CONSIDERED

From the large variety of airfoils, 15 airfoils were selected on the basis of the availability of wind-tunnel test data, which was facilitated by the on-going Low-Speed Airfoil Test program at the University of Illinois at Urbana-Champaign.[6-8] These airfoils are depicted in Figure 1 each with their respective relative thickness. With the exception of the Clark-Y and NACA 2414 (which represent here the traditional airfoils) and the Göttingen 417a (Go417a), all of the remaining airfoils were specifically designed for low Reynolds number applications. Moreover, among the latter airfoils, only the BW-3 airfoil and the NREL S822/S823 thick airfoil family[2] were developed specifically for wind turbine applications while the others have been mainly used for unmanned aerial vehicle applications. For the NREL S822 and S823 airfoils, the S822 is for the tip and the S823 is for the root of the blade. It is also noteworthy that the BW-3 airfoil was developed by Bergey Wind Power and is used on their 7-m diameter Excel Wind Turbine System, having a rated power of 10 kW.

4. WIND-TUNNEL TESTING APPARATUS AND METHOD

The airfoil data was obtained from wind-tunnel experiments performed in the University of Illinois at Urbana-Champaign (UIUC) low-turbulence subsonic wind tunnel. It is an open-return tunnel with a test section that is 0.857 m (2.813 ft) high and 1.219 m (4 ft) wide. The 0.305 m (12 in) chord models were mounted horizontally between two 1.829 m (6 ft) long Plexiglass splitter plates spaced 0.854 m (2.802 ft) apart. Gaps between the model and the splitter plates were nominally 1-2 mm (0.004-0.008 in).

The freestream velocity was obtained from dynamic pressure measurements obtained with a static-pitot tube placed between the splitter plates and about one chord length ahead of the airfoil model. These measurements were corrected for solid and wake blockage, as well as for circulation and boundary-layer growth effects.[6,14] The turbulence intensity of the empty test section of the tunnel was less than 0.1%[15] for the Reynolds number range of the tests, which varied from 60,000 to 500,000 depending on the airfoil tested. Lift was directly measured using a strain gage load cell[8] having an accuracy and repeatability of 0.01% of the rated output.
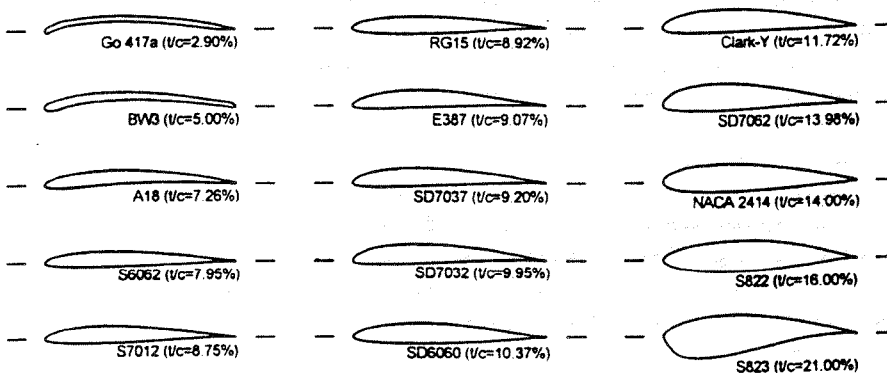

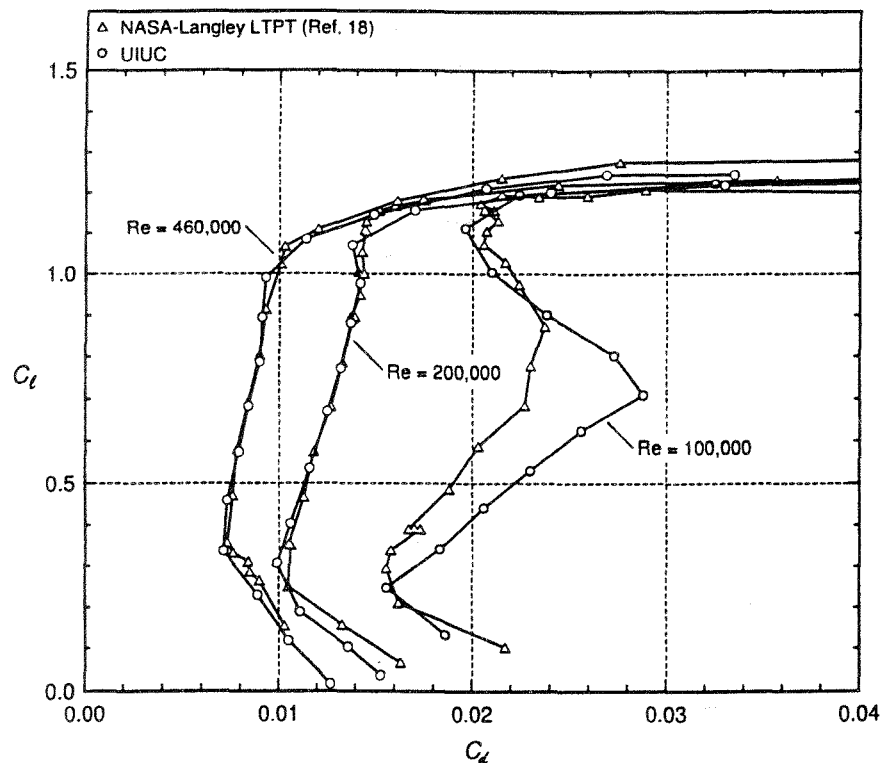Figure 1.   The airfoils considered.

Figure 2.   Comparison between the data obtained at UIUC and NASA Langley LTPT for the
Eppler 387 airfoil.

The drag was determined from the average of four different spanwise wake surveys spaced
76.2 mm (3 in) apart and 1.5 chord length behind the training edge of the model. The lift and
drag measurements were also corrected for wind tunnel interference effects. The overall cor-
rection method was validated from tests with the Eppler 387 airfoil. As shown in Figure 2, the
lift and drag data obtained at UIUC agree with the results from the Langley Low Turbulence
Pressure Tunnel (LTPT).[14.18] The agreement is particularly good for Reynolds numbers of
200,000 and 460,000 and fair at 100,000 taking into account the overall uncertainty of 1.5%
on both the lift and drag measurements. Furthermore, the accuracy of the wind tunnel models
tested was within 0.25 mm (0.010 in) of the nominal coordinates and was 0.10 mm (0.004 in)
in the case of the Eppler 387 airfoil model. More detailed information about the wind tunnel as
well as the measurement and correction techniques can be found in References 6, 7 and 14.

The method used to simulate leading-edge roughness on the airfoils was to fix a 0.58 mm
(0.023 in) thick zigzag trip at 2% chord on the upper surface and 5% chord on the lower
surface (10% chord in the case of the S823 airfoil). The trips promote early transition that
takes place slowly over a considerable distance along the airfoil.[13] The results simulating rough-
ness effects are referred to as the data for fixed transition as opposed to the results for free
transition (clean conditions). These results for fixed transition should be considered as a worst
case scenario. Therefore, if the C_{lmax} of an airfoil is not significantly affected by the addition of
the trips, then it is said to be C_{lmax} roughness insensitive.

5. EXPERIMENTAL RESULTS

The drag polars for the airfoils considered are presented in Figure 3 (results for free transition).
Data is shown in the Reynolds number range of 60,000 to 500,000 which is representative of
performance at lower and higher Reynolds numbers since the drag typically varies the most
below a Reynolds number of 300,000. As expected, the overall drag of the thicker airfoils is
generally higher than that of the thinner airfoils, especially at a Reynolds number of 100,000.
The S822 and S823, which at 16% and 21% thick are the two thickest airfoils considered, show
indeed higher drag than the other airfoils. For these thick airfoils, laminar separation effects are
particularly severe at Reynolds numbers of 100,000 and below. For the S822 airfoil, which was

designed for a Reynolds number of 600,000 as compared with 400,000 for the S823 airfoil, signs of a laminar separation bubble can be also seen at Reynolds numbers up to 300,000. Consequently, the important structural advantages provided by a high relative airfoil thickness come with a significant penalty in aerodynamic performance at low Reynolds numbers.

As shown in Figure 3, not only the S822 and S823 airfoils but most of the airfoils considered have drag polars that indicate the presence of a laminar separation bubble at a Reynolds number of 100,000. At this Reynolds number, the drag polars of the A18, BW-3, Go417a, S7012 and SD7037, which are among the thinnest airfoils considered, indicate rather small laminar separation effects as compared with the other airfoils. In general, thin airfoils perform best at low Reynolds numbers as the pressure recovery is not as steep as compared with thick airfoils. Particularly, thin airfoils such as the Go417a and the BW-3, have distinctive drag polars. These two airfoils have a particularly narrow lift range for low drag (drag bucket) that is a consequence of their low thickness.

For wind turbine applications, the influence of leading-edge roughness is important in evaluating the potential of an airfoil for wind turbine applications. Similarly to the data for free transition, the drag polars of the airfoils tested with simulated leading-edge roughness are shown in Figure 4. As expected, the addition of trips caused an overall increase in drag except for the airfoils that suffered from severe laminar separation effects under clean conditions. Also, the drag polars show that for fixed transition the performance is essentially Reynolds number independent as the drag polars fall nearly on a single curve. The zigzag trips located at the leading-edge quickly produce a turbulent boundary layer and the drag for a given airfoil is consequently not especially sensitive to the Reynolds number.

Lift data illustrating the stall characteristics of the airfoils is shown in Figure 5 for a Reynolds number of 300,000. Figure 5 also presents results for fixed transition for those airfoils tested with simulated leading-edge roughness. As indicated in Figure 5, the C_{lmax} of the A18, BW-3, S822, S823, S7012 and SD7037 airfoils are not particularly sensitive to roughness. For Reynolds numbers of 300,000 and above, lift hysteresis is typically not present on low Reynolds number airfoils, and consequently the lift data in Figure 5 was only shown for increasing angle of attack. From the airfoils tested, only the NACA 2414 has a lift hysteresis loop at a Reynolds number of 300,000.[5] As mentioned previously, lift hysteresis is related to the presence of a laminar separation bubble. Therefore, lift hysteresis is more severe at Reynolds numbers below 200,000 and is not present when the flow is tripped as in the case of simulated leading-edge roughness. At Reynolds numbers below 200,000, the Clark-Y, NACA 2414, and SD7062 airfoils have significant lift hysteresis.[6-8]

Table 1. Performance parameters for the airfoils considered for free and fixed transition at $Re = 300,000$.

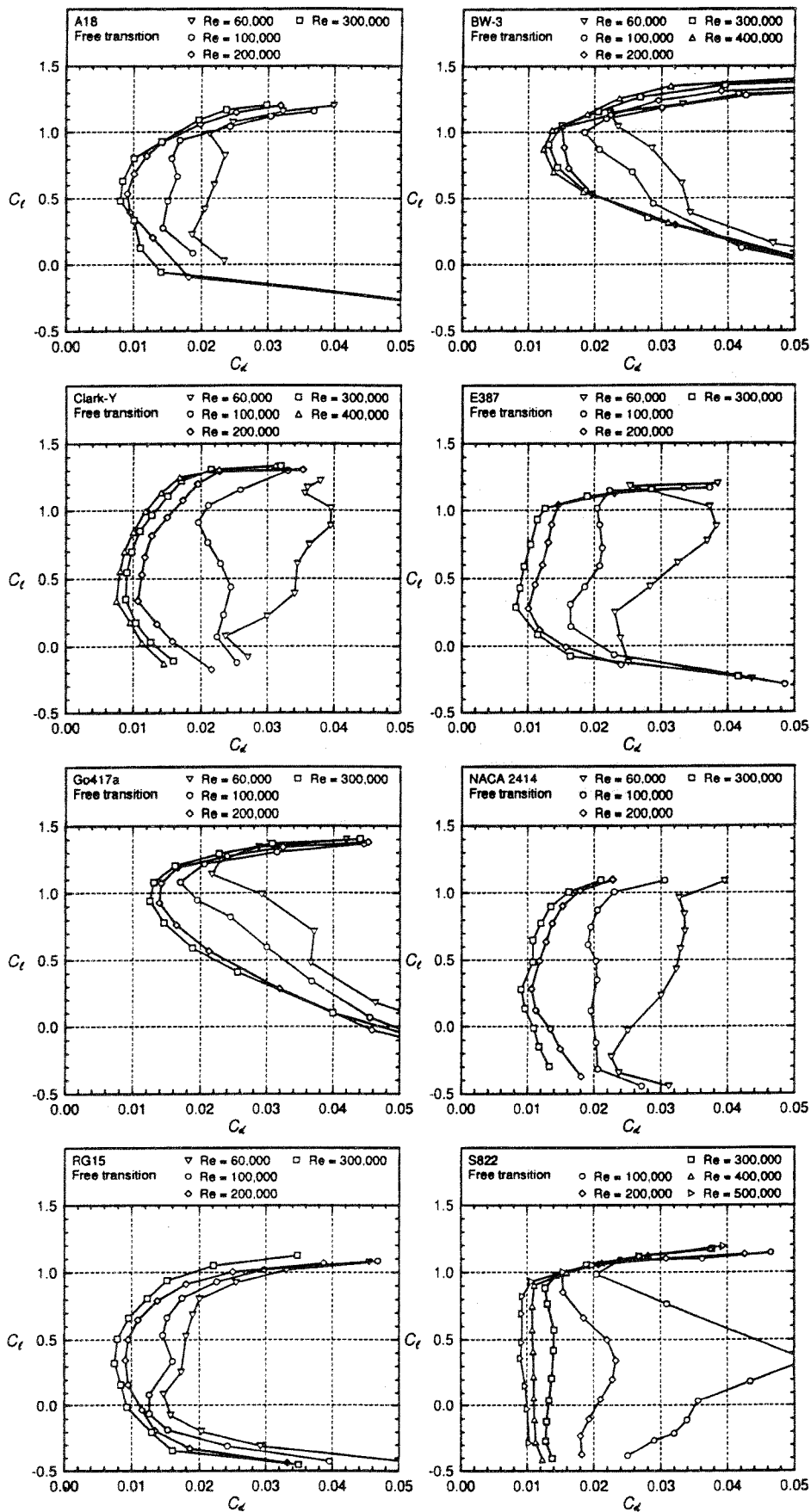| Airfoil	Free transition			Fixed transition			Percentage Difference	
	$(C_l/C_d)_{max}$	C_l	C_{lmax}	$(C_l/C_d)_{max}$	C_l	C_{lmax}	$(C_l/C_d)_{max}$	C_{lmax}
A18	79.6	0.80	1.23	41.2	1.03	1.22	48.2	0.7
BW-3	69.6	1.05	1.44	39.6	0.89	1.41	43.1	1.9
Clark-Y	77.2	0.85	1.35	39.1	0.83	1.13	49.4	16.5
E387	81.7	0.93	1.29	–	–	–	–	–
Go471a	82.3	1.08	1.40	–	–	–	–	–
NACA2414	66.6	0.90	1.23	–	–	–	–	–
RG15	69.0	0.66	1.14	–	–	–	–	–
S822	69.4	0.88	1.22	32.9	0.68	1.18	52.6	3.8
S823	62.7	1.05	1.18	30.2	0.78	1.14	51:8	3.0
S6062	73.1	0.65	1.11	–	–	–	–	–
S7012	72.1	0.71	1.14	40.4	0.94	1.15	44.0	–0.7
SD6060	73.5	0.72	1.11	–	–	–	–	–
SD7032	83.4	1.00	1.39	–	–	–	–	–
SD7037	76.3	0.84	1.28	44.1	0.99	1.32	42.2	–3.1
SD7062	77.5	1.23	1.66	45.1	0.96	1.23	41.8	25.8

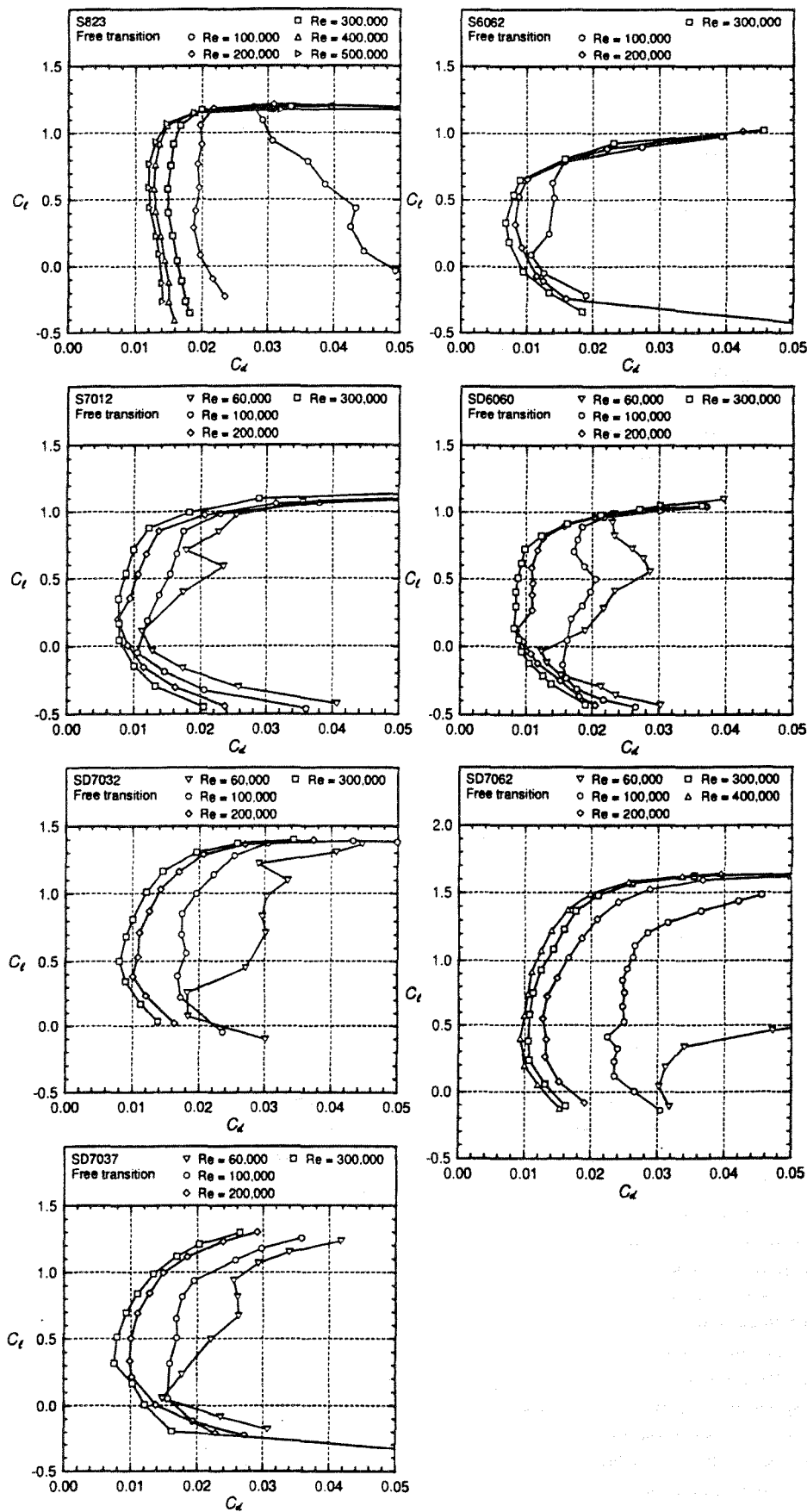Figure 3.   Drag polars for the airfoils considered (free transition).

Figure 3 cont.   Drag polars for the airfoils considered (free transition).

The performances of the 15 airfoils considered at a Reynolds number of 300,000 are summarized in Table 1, which gives the maximum lift-to-drag ratio of the airfoils and corresponding lift coefficient, and the maximum lift coefficient for both free and fixed transition. As an indication of the sensitivity of each airfoil to leading-edge roughness on the maximum lift-to-drag ratio and maximum lift coefficient, the percentage difference between the results for free and fixed transition is also indicated. The importance of the results presented in Table 1 depends on the type of wind turbine considered. The next section focuses on the interpretation of the results and classification of the airfoils considered.

6. AIRFOIL SELECTION

From the airfoil data presented in the previous section, it is now possible to establish general and specific guidelines for the selection of appropriate airfoils for the design of small HAWTs. The specific guidelines are subdivided according to the different types of HAWTs – variable-speed, variable-pitch, and stall regulated. Note that these guidelines can also be used for the design of new airfoils for small HAWTs. Before considering in detail each of the three types of HAWTs, some general comments about selecting the most suitable airfoil(s) for a particular wind turbine are provided.

The first step in the airfoil selection process is to estimate the Reynolds number range over which the blades will operate. This step applies to any size HAWT but is particularly important for small wind turbines because of the wide variation in drag at low Reynolds numbers. The expression for the chord Reynolds number on a wind turbine blade is given by

$$Re = \frac{c\sqrt{[V_\infty(1-a)]^2 + [\Omega r]^2}}{\nu} \tag{1}$$

For the case of a variable-speed wind turbine, the rotational component Ωr is typically much greater than the freestream velocity, thus the Reynolds number can be approximated by

$$Re = \frac{V_\infty TSR\ (r/R)c}{\nu} \tag{2}$$

where TSR is the tip-speed ratio. For stall-regulated wind turbines, the general expression (1) cannot be simplified.

Once the operational Reynolds number range is known for a particular rotor, the shape of the drag polars at the Reynolds numbers of interest is a key element in the classification of airfoils for the different types of wind turbines. Drag polar characteristics, such as the maximum lift-to-drag ratio and corresponding lift coefficient, and the size of drag bucket are important features in evaluating the potential of an airfoil for wind turbine applications under design and off-design conditions. For wind turbines that operate up to and beyond stall, the maximum lift coefficient is another important parameter to consider. As seen in Figures 4 and 5, roughness effects significantly increase the overall drag and can also negatively affect the lift characteristics and thus aerodynamic performance with simulated leading-edge roughness is likely to be useful in the airfoil selecting process.

Finally, it is important to note that the use of lift and drag data at constant Reynolds numbers can be misleading in selecting an airfoil. This can be explained by the effect of the inverse relationship between chord length and lift coefficient for a given blade load along the span. With all else equal, a blade operating at high lift coefficients will have a relatively low solidity and thus, the blade will operate at lower Reynolds numbers as compared with another blade operating at lower lift coefficients. This trade-off between operating lift coefficient and Reynolds number is of particular significance for small HAWTs because of the large drag variations at low Reynolds numbers. Furthermore, the inverse relationship between lift coefficient and Reynolds number is more critical for variable-speed HAWTs because their operational Reynolds number range is typically much larger than that of constant-speed wind turbines. For variable-speed wind turbines, this inverse relationship can be expressed through the so-called reduced Reynolds number to be discussed in the next section.
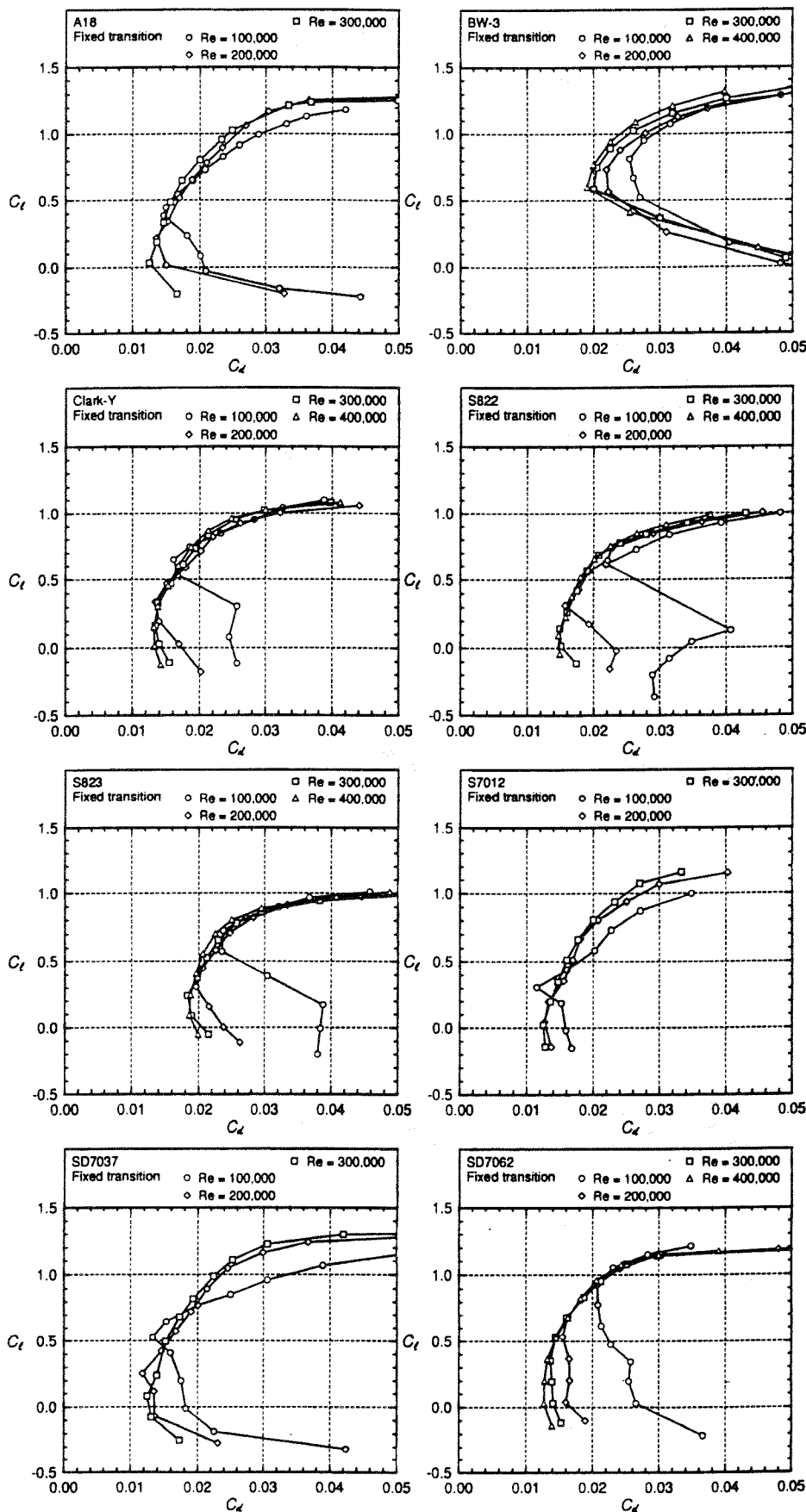
Figure 4.   Drag polars for the airfoils tested with simulated leading-edge roughness (fixed transition).
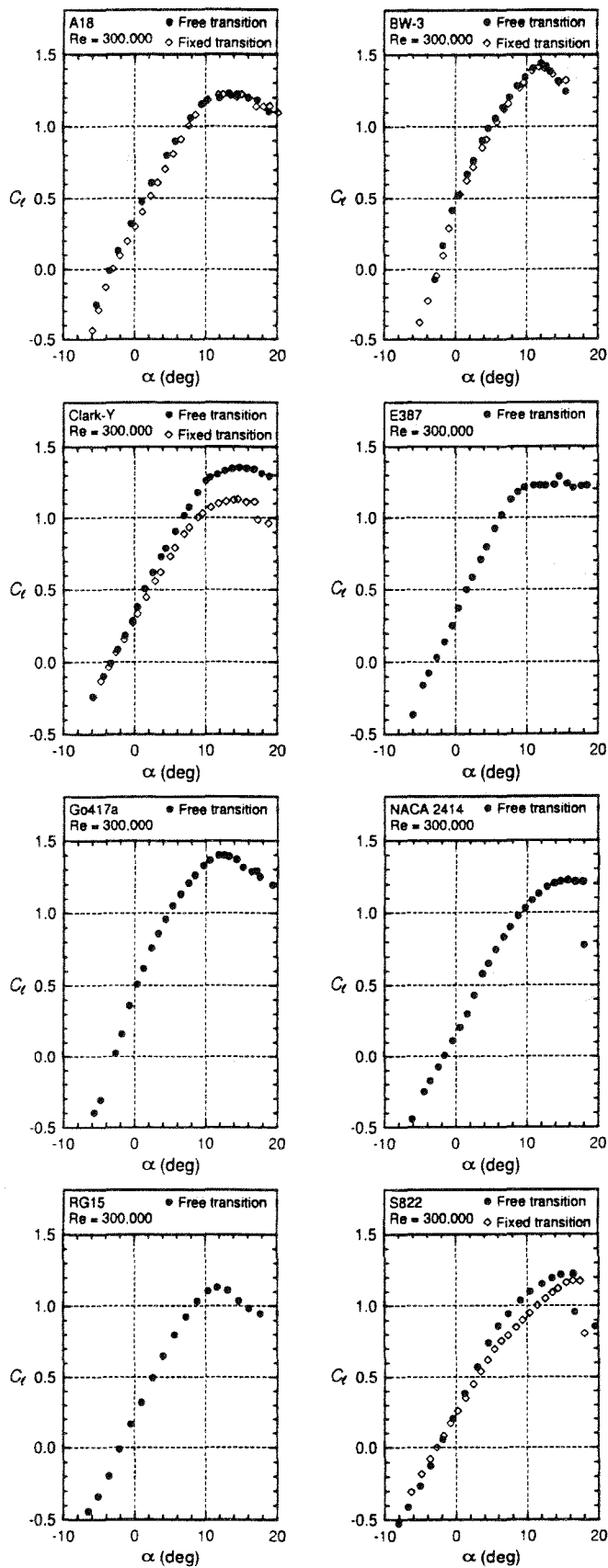
Figure 5. Lift curves for the airfoils considered at $Re = 300,000$ (fixed transition).
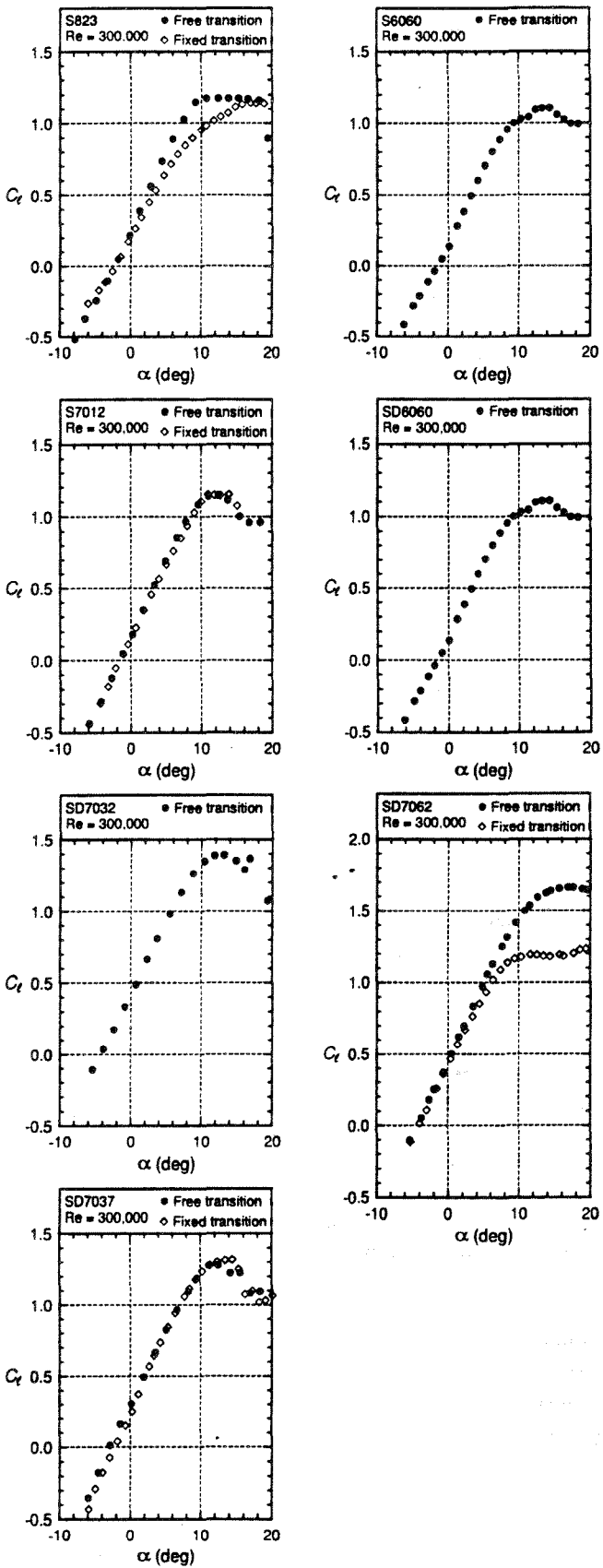
Figure 5 cont. Lift curves for the airfoils considered at Re = 300,000 (fixed transition).

6.1 Airfoils for Variable-Speed HAWTs

Under normal conditions, variable-speed HAWTs ideally operate at constant *TSR*, and thus each blade station operates at a constant angle of attack. The lift coefficient at each blade station is then constant and accordingly, the blade can be set to operate at the angle of attack or lift coefficient that maximizes the lift-to-drag ratio at that station. Consequently, the airfoil selection process for variable-speed HAWTs can be mainly based on maximum lift-to-drag ratio characteristics.

There is usually a trade-off between the size of the drag bucket and the maximum lift-to-drag ratio of an airfoil. Higher lift-to-drag ratios can be achieved at the cost of a narrower drag bucket. For variable-speed operations, that is acceptable since the operating lift coefficient is ideally constant. For optimum aerodynamic performance, airfoils tailored for variable-speed HAWTs can be designed with aft camber to unload the upper surface, thereby reducing the strength of the suction side adverse pressure gradient which results in decreased drag at the cost of a narrower drag bucket. Practically, however, one must also account for off-design conditions caused by fluctuations in the *TSR* owing to atmospheric turbulence. Off-design conditions can also be caused by roughness effects from erosion and accumulation of airborne contaminates such as insects, but for variable-speed HAWTs these effects are not as critical as for constant-speed wind turbines, particularly stall regulated HAWTs.[2,16] Airfoils with a small drag bucket will generally maximize performance under the design conditions while those with a wider drag bucket will be less affected by off-design conditions. Consequently, the selection of the airfoil(s) should also account for the ability of the power electronics to keep the *TSR* constant.

In selecting an airfoil for a variable-speed HAWT, data for constant Reynolds numbers should be interpreted with care. The lift coefficient for maximum lift-to-drag ratio depends on the chord length which impacts the Reynolds number, and thus the distribution of the lift-to-drag ratio along the blade will vary. It is well known that for a given blade station, wind speed, and axial inflow, the product of the blade solidity and the lift coefficient is a constant, viz

$$\sigma C_l = \text{constant} \qquad (3)$$

Isolating the chord in the expression for the blade solidity and combining with the general expression for the Reynolds number gives[17]

$$\Re = Re C_l \qquad (4)$$

where $\Re$ is termed the reduced Reynolds number.

Briefly, the reduced Reynolds number $\Re$ is constant for a given blade station as long as the *TSR*, *V* and *a* are constant. The reduced Reynolds number distribution along the blade can be determined by setting the *TSR* and V_∞ as well as the *a* and C_l distributions. Once determined, the reduced Reynolds number for a particular blade station is independent of a change in C_l so long as the blade loading remains the same, thereby leading to similar power output characteristics. The problem is to find the optimum reduced Reynolds number which maximizes the value of the lift-to-drag ratio.

Knowledge of the airfoil performance with simulated leading-edge roughness is particularly useful for variable-speed HAWTs that control peak power by furling, because one side of the rotor disk is likely to stall during furling. Consequently, reduced roughness sensitivity may provide consistent furling characteristics and as a result cause minimal cyclic blade loads. It should be added that airfoils having gentle stall characteristics should be favored for furling wind turbines.

6.2 Airfoils for Variable-Pitch HAWTs

In contrast to variable-speed wind turbines, those operating at constant speed, such as variable-pitch HAWTs, have their blades operating over a broad lift range. Before pitch control is activated, the angle of attack of a given blade station increases with increasing windspeed. Accordingly, airfoils for variable-pitch HAWTs should have a wide lift range for low drag to maximize energy capture. This wide drag bucket requirement is, however, less critical for

wind turbines that have more than one speed setting for which constant-speed operation can be maintained. With the exception of the BW-3 and Go417a airfoils, which have a narrow drag bucket, the remaining airfoils that were tested offer a wide selection for constant-speed HAWTs. These airfoils span a wide range of thickness with the S822 and S823 airfoils being the best candidates if high thickness is required. Note, however, that if thick airfoils are used at the root of small HAWTs, it might be preferable to extend the hub until the chord Reynolds number is near 100,000 to 200,000 because of the typically poor aerodynamic performance of thick airfoils below those Reynolds numbers.

6.3 Airfoils for Stall Regulated HAWTs

The airfoil requirements for small stall-regulated HAWTs are the same as those for variable-pitch HAWTs. There is, however, one additional and critical requirement for wind turbines that have their blades stall to regulate power. The airfoils used on stall-regulated wind turbines should be $C_{l_{max}}$ insensitive to roughness in order to minimize the loss in peak power owing to roughness effects. From the airfoils tested with simulated leading-edge roughness, the A18, BW-3, S7012, S822, S823, and SD7037 airfoils are essentially $C_{l_{max}}$ insensitive to roughness and therefore, are applicable to stall regulated HAWTs. As previously mentioned, however, the BW-3 airfoil is likely not to yield optimum performance for constant-speed wind turbines owing to its narrow drag bucket.

7. SUMMARY

As a result of wind tunnel tests conducted in the same facility under the same conditions, a consistent airfoil performance database of 15 low Reynolds number airfoils is now available. Data was taken for clean-blade conditions and with simulated leading-edge roughness. Such data sets can be used in wind turbine performance tradeoff and design studies of small HAWTs. The concept of the reduced Reynolds number (as contrasted with the traditional Reynolds number) was introduced for variable-speed machines to show the tradeoff between the blade operating lift coefficient and the resulting chord length which directly impacts the Reynolds number. Some guidelines were provided for use in the airfoil selection process for stall-regulated, variable-pitch and variable-speed HAWTs. These guidelines, which are based on desirable drag-polar and lift-curve characteristics, can also be used in the design of new airfoils for small blades. Furthermore, some of these guidelines are also applicable to larger size wind turbines.

REFERENCES

1. **Abbott, I.H. and Doenhoff, A.E.** *(1959)* *"Theory of Wing Sections"*, *Dover Publications, New York.*

2. **Tangler, J.L. and Somers, D.M.** *(1995)* *"NREL Airfoil Families for HAWTs"*, *American Wind Energy Association Wind Power '95 Conference, May 9–12, Washington, DC.*

3. **Giguère, P. and Selig, M.S.** *(1997)* *"New Airfoils for Small HAWTs"*, *Wind Power '97 Conference, Austin, TX, June 16–18, 1997 (also accepted for publication in the ASME Journal of Solar Energy Engineering).*

4. **Althaus, D.** *(1980)* *"Profilpolaren Für Den Modellflug (Band 1 and 2)"*, *N.V. Neckar Verlag.*

5. **Selig, M.S., Donovan, J.F. and Fraser, D.B.** *(1989)* *"Airfoils at Low Speeds"*, *SoarTech*

8, SoarTech Publications, 1504 N. Horseshoe Circle, Virginia Beach, Virginia 23451, USA.

6. Selig, M.S., Guglielmo, J.J., Broeren, A.P. and Giguère, P. *(1995)* *"Summary of Low-Speed Airfoil Data – Volume 1"*, SoarTech Publications, 1504 N. Horseshoe Circle, Virginia Beach, Virginia 23451, USA.

7. Selig, M.S., Lyon, C.A., Giguère, P., Ninham, C.P. and Guglielmo, J.J. *(1996)* *"Summary of Low-Speed Airfoil Data – Volume 2"*, SoarTech Publications, 1504 N. Horseshoe Circle, Virginia Beach, Virginia 23451, USA.

8. Lyon, C.A., Broeren, A.P., Giguère, P., Gopalarathnam, A. and Selig, M.S. *(1997)* *"Summary of Low-Speed Airfoil Data – Volume 3"*, SoarTech Publications, 1504 N. Horseshoe Circle, Virginia Beach, Virginia 23451, USA.

9. Mueller, T.J. *(1985)* *"Low Reynolds Number Vehicles"*, AGARDograph No. 288.

10. Marchman, J.F. *(1987)* *"Aerodynamic Testing at Low Reynolds Numbers"*, Journal of Aircraft, Vol. 24, No. 2, pp. 107–114.

11. Drela, M. *(1989)* *"XFOIL: An Analysis and Design System for Low Reynolds Number Airfoils"*, Lecture Notes in Engineering: Low Reynolds Number Aerodynamics, T.J. Mueller (ed), Vol. 54, Springer-Verlag, new York, June 1989.

12. Carmichael, B.H. *(1981)* *"Low Reynolds Number Airfoil Survey"*, NASA Contractor Report 165803, November 1981.

13. Lyon, C.A., Selig, M.S. and Broeren, A.P. *(1997)* *"Boundary-Layer Trips on Airfoils at Low Reynolds Numbers"*, AIAA paper 97-0511.

14. Giguère, P. and Selig, M.S. *(1997)* *"Velocity Correction for Two Dimensional Tests with Splitter Plates"*, AIAA Journal, Vol. 35, No. 7, pp. 1195–1200.

15. Guglielmo, J.J. *(1996)* *"Spanwise Drag Variations at Low Reynolds Numbers"*, Masters Thesis, Department of Aeronautical and Astronautical Engineering, University of Illinois at Urbana-Champaign, May 1996.

16. Tangler, J.L. *(1997)* *"Influence of Pitch, Twist and Taper on a Blade's Performance Loss Due to Roughness"*. ASME Journal of Solar Energy Engineering, Vol. 119, August 1997, pp. 248–252.

17. Giguère, P. and Selig, M.S. *(1997)* *"Desirable Airfoil Characteristics for Large Variable-Speed Horizontal Axis Wind Turbines"*, ASME Journal of Solar Energy Engineering, Vol. 119, August 1997, pp. 253–260.

18. McGhee, R.J., Jones, G.S. and Jouty, R. *(1988)* *"Performance Characteristics from Wind-Tunnel Tests of a Low Reynolds Number Airfoil"*, AIAA Paper 88-0607, January 1988.